



ARTICLE

Alterations in microbiome composition and metabolic byproducts drive behavioral and transcriptional responses to morphine

Rebecca S. Hofford^{1,2}, Nicholas L. Mervosh^{1,2}, Tanner J. Euston^{1,2}, Katherine R. Meckel^{2,3}, Amon T. Orr^{1,2} and Drew D. Kiraly^{1,2,3,4}

Recent evidence has demonstrated that the gut microbiome has marked effects on neuronal function and behavior. Disturbances to microbial populations within the gut have been linked to myriad models of neuropsychiatric disorders. However, the role of the microbiome in substance use disorders remains understudied. Here we show that male mice with their gut microbiome depleted by nonabsorbable antibiotics (Abx) exhibit decreased formation of morphine conditioned place preference across a range of doses (2.5–15 mg/kg), have decreased locomotor sensitization to morphine, and demonstrate marked changes in gene expression within the nucleus accumbens (NAc) in response to high-dose morphine (20 mg/kg × 7 days). Replacement of short-chain fatty acid (SCFA) metabolites, which are reduced by microbiome knockdown, reversed the behavioral and transcriptional effects of microbiome depletion. This identifies SCFA as the crucial mediators of microbiome–brain communication responsible for the effects on morphine reward caused by microbiome knockdown. These studies add important new behavioral, molecular, and mechanistic insight to the role of gut–brain signaling in substance use disorders.

Neuropsychopharmacology (2021) 46:2062–2072; <https://doi.org/10.1038/s41386-021-01043-0>

INTRODUCTION

Opioid use disorder (OUD) is a devastating neuropsychiatric condition that leads to tremendous hardship for patients and families alike. In recent years overdose deaths from opioids have continued to rise, accounting for almost 70,000 lives lost last year in the United States alone [1, 2]. The current state of the art treatment for OUD is the use of opioid agonist replacement therapies. While these therapies can be quite effective for some [3], for too many patients they are ineffective or unpalatable. Additionally, they are associated with often intolerable side effects and carry the potential for dependence [4] which can decrease compliance and contribute to relapse [5]. For this reason, pharmaceuticals and interventions focusing on non-traditional targets have gained interest as potential treatments or mitigation strategies for OUD.

Over the last decade, there has been increased interest in the resident population of bacteria in the intestinal tract, collectively called the gut microbiome, as a mediator of neuropsychiatric disease [6, 7]. Individuals with autism spectrum disorder [8], major depression [9], and other neuropsychiatric conditions [10, 11] exhibit significantly disrupted gut microbial populations. While most clinical work is currently observational, preclinical studies have begun to clarify the mechanism of microbiome–brain crosstalk in neuropsychiatric disease. Based on this early work, the presence of a complete and diverse microbiome is necessary for normal brain function and behavior. Mice born germ-free (i.e., without any internal or external microbiome) exhibit alterations in anxiety-like and social behaviors [12, 13] as well as dysregulation

of gene expression and chromatin structure in the brain [14, 15]. Adult mice with their microbiome depleted with antibiotics exhibit changes in fear learning [16, 17], behavioral response to cocaine [18], and corresponding transcriptional control in limbic brain regions [16–18].

While there are multiple potential routes of gut–brain communication [19], one of the best studied is via the production of neuroactive metabolites by the microbiome. One class of metabolite, the short-chain fatty acids (SCFA), which are formed by bacterial fermentation of dietary fiber [20], have garnered particular interest as gut–brain signaling molecules. These molecules pass from the intestine into blood, can cross the blood–brain barrier [21], and have been shown to affect development of neurodegeneration [22], models of autism [23], and behavioral response to cocaine [18]. SCFA serve a variety of cellular functions and can act as histone deacetylase (HDAC) inhibitors [24], serve as sources for histone acylations [25, 26], have direct effects on transcription factor activity [27–30], and can signal via the vagus nerve retrograde to the CNS in ways that drive behavior [31–33], among other potential cellular mechanisms [34]. Given these myriad of potential cellular mechanisms, and the known effects on brain and behavior in multiple models of neuropsychiatric disease, the SCFA are positioned as a target of great mechanistic interest in the gut–brain axis.

Recently, our group demonstrated that alterations in the gut microbiome and SCFA influence drug reward for cocaine [18]. Reduction in the total number of bacteria and microbiome diversity through the addition of broad-spectrum antibiotics (Abx)

¹Department of Psychiatry, Icahn School of Medicine at Mount Sinai, New York, NY, USA; ²Friedman Brain Institute, Icahn School of Medicine at Mount Sinai, New York, NY, USA; ³Nash Family Department of Neuroscience, Icahn School of Medicine at Mount Sinai, New York, NY, USA and ⁴The Seaver Center for Autism Research and Treatment, Icahn School of Medicine at Mount Sinai, New York, NY, USA

Correspondence: Drew D. Kiraly (drew.kiraly@mssm.edu)

Received: 8 December 2020 Revised: 23 April 2021 Accepted: 12 May 2021

Published online: 14 June 2021

into drinking H₂O enhances cocaine conditioned place preference (CPP) at low doses [18], and repleting SCFA concurrent with Abx returns place preference to baseline levels. Additional work demonstrated that the combination of opioids and gut microbiome disturbance can also affect cocaine reward [35]. Several other studies have examined connections between the microbiome and response to opioids. Germ-free mice or mice with their microbiome knocked down via oral Abx do not develop tolerance to the antinociceptive effects of morphine [36, 37]; this effect is reversed by colonization of the gut with a microbiome from healthy mice [36]. Additionally, Abx has been shown to disrupt the neuronal ensembles normally activated by oxycodone administration and withdrawal [38], suggesting that the microbiome mediates opioids' effects on both behavior and brain function. However, it is currently unclear if microbiome depletion directly affects the rewarding properties of opioids [7].

The studies herein present the first direct test of the relationship between the gut microbiome and opioid reward using an oral antibiotic knockdown model. We find that mice lacking a complex microbiome have decreased development of preference for and sensitization to morphine. Additionally, we see that mice with a depleted microbiome have markedly different transcriptional responses in the nucleus accumbens (NAc) following opioid treatment. Finally, we see that repletion of SCFA metabolites to antibiotic treated mice reverses behavioral and transcriptional effects of microbiome depletion. Taken together, our findings provide evidence for a role of the microbiome in addiction-like behaviors and provide mechanistic insight into gut-brain signaling pathways.

MATERIALS AND METHODS

Animals

Male C57BL/6 mice (7–9 weeks old, Jackson Laboratories) were group-housed (4–5 mice/cage) in a humidity and temperature-controlled colony room on a 24 h light–dark cycle (lights on at 7:00). Drink solutions and food were available ad libitum throughout the entirety of all experiments. All animal procedures were approved by the Mount Sinai IACUC and all procedures conformed to the “Guide for the Care and Use of Laboratory Animals” (National Research Council 2010).

Preparation and delivery of drink solutions

Cages were randomly assigned to H₂O, Abx, SCFA, or SCFA + Abx conditions, depending on experiment. Abx cocktail contained 0.5 mg/ml vancomycin (Chem-Impex International #00315), 2 mg/ml neomycin (Fisher Scientific #BP266925), 0.5 mg/ml bacitracin (Research Products International #B3200025), and 1.2 µg/ml pimaricin (Infodine Chemical #7681-93-8) in H₂O. SCFA solution contained 40 mM butyrate (#303410), 25.9 mM propionate (#P1880), and 67.5 mM acetate (#S5636) in H₂O (all SCFA purchased from Sigma Aldrich); SCFA + Abx was a combination of the two drink solutions at the same final concentrations of each compound. Mice from all groups were treated with their respective drink solutions 2 weeks before the start of experimental procedures and remained on treatment until the conclusion of the study. Mice were weighed before placement on drink solutions and no less than once weekly thereafter.

Morphine

Morphine sulfate was provided by the NIDA drug supply program from National Institute on Drug Abuse and was diluted in saline and injected at a volume of 10 ml/kg.

16S sequencing

Mice from H₂O or Abx cages were given once daily injections of 20 mg/kg morphine or saline (s.c.) for 7 days and were rapidly decapitated 24 h after their last injection. Caecal contents were

removed, flash frozen on dry ice, and stored at –80 °C. DNA from caecal contents were isolated using DNeasy PowerSoil Kit (Qiagen) following kit instructions with an extended bead beating step. DNA concentration was determined with a NanoDrop1000. PCR amplification was achieved using primers (341F/805R) targeting the V3 and V4 region of the 16S rRNA region of the bacterial genome and was sequenced on an Illumina NovaSeq (2 × 250 bp paired-end). Amplicons were chimera filtered, dereplicated, and paired-ends were merged using Divisive Amplicon Denoising Algorithm 2 [39], which identified unique genomic features. These features were used to determine observed taxonomic units (OTU), defined as sequences with ≥97% similarity. OTU counts were used to determine the Shannon index of alpha diversity and principle coordinates analysis plots were generated using the Unifrac distance as an assessment of beta diversity using QIIME2 software [40]. OTUs were identified by comparing their genetic sequences to reference bacterial genomes using SILVA (Release 132) [41] with confidence set to 0.7.

Detection of SCFA levels

To quantify caecal SCFA mice were placed on Abx or kept on H₂O for 2 weeks before rapid decapitation and removal of caecal contents as described above ($n = 4–5$ /group). SCFAs were quantified using a Water Acquity uPLC System with a Photodiode Array Detector using standard methods from the UPenn metabolomics center (details in Supplementary Methods).

Locomotor sensitization

Mice from H₂O or Abx cages ($n = 5$ /group) were assessed for their locomotor response to repeated morphine using San Diego Instruments Photobeam Activity System. The locomotor arena consisted of a frame crossed with infrared beams in the x and y dimensions. Clean, empty rat cages were placed within this frame to contain the mice while simultaneously allowing penetration of the infrared beams. Mice could freely move throughout the space and infrared beam breaks were counted to determine locomotor activity. Abx and H₂O mice were injected with 10 mg/kg morphine (s.c.) and were allowed to ambulate for 45 min. This occurred once daily for 5 days. Ten days after the last morphine injection, mice were given a morphine challenge injection and were placed back into the locomotor arena to measure persistence of morphine locomotor sensitization.

Morphine conditioned place preference

Mice from H₂O, Abx, SCFA, or SCFA + Abx ($n = 5–10$ /group) underwent morphine CPP as described previously [18] using Med Associates automated boxes and software. Detailed methods in Supplementary Methods.

RNA-sequencing of NAc

H₂O and Abx mice (same mice used for 16S sequencing, $n = 5$ /group) were given once daily injections of 20 mg/kg morphine or saline (s.c.) for 7 days and were rapidly decapitated 24 h after their last injection. NAc was identified by the anterior commissure and removed using a 14 gauge blunt needle. NAc punches were flash frozen on dry ice and stored at –80 °C. RNA was extracted from the tissue using Trizol according to standard procedures. The integrity and purity of total RNA were assessed using Agilent Bioanalyzer and OD260/280 using Nanodrop. cDNA was generated using Clontech SMARTer cDNA kit (Clontech Laboratories, Inc., Mountain View, CA USA, catalog# 634925) from total RNA. cDNA was fragmented using Bioruptor (Diagenode, Inc., Denville, NJ USA), profiled using Agilent Bioanalyzer, and subjected to Illumina library preparation using SPRIworks HT Reagent Kit (Beckman Coulter, Inc. Indianapolis, IN USA, catalog# B06938). The quality and quantity and the size distribution of the Illumina libraries were determined using an Agilent Bioanalyzer 2100. The samples were then sequenced on an Illumina HiSeq2500

which generated paired-end reads of 106 nucleotides (nt). Data generated and checked for data quality using FASTQC (Babraham Institute, Cambridge, UK).

RNA-sequencing bioinformatics

The raw RNASeq reads (Fastq files) for each sample were aligned to the *Mus musculus* 10 reference genome (https://www.ncbi.nlm.nih.gov/assembly/GCA_001269945.2) using STAR v2.4.0 [42] with default parameters, using the DNAnexus platform. After alignment, estimation of transcript abundance measures as fragments per kilobase of exon per million aligned fragments (FPKM) values was performed using Cufflinks in the Tuxedo protocol, and FPKM values were used for generation of all heatmaps. For pairwise comparisons aligned reads were then analyzed for differential gene expression utilizing the limma software package [43] run through the BioJupies analysis package with default parameters [44]. Statistical significance was set at a threshold of FDR-corrected $p < 0.05$. Significantly regulated gene lists were separately entered into G:Profiler [45], and significantly regulated pathways were identified using an FDR corrected $p < 0.05$. Further details available in Supplementary Methods.

Statistical analysis

Statistical significance for OTU and Shannon index were analyzed using a 2×2 between-subjects ANOVA with drug treatment and drink type as fixed factors. To determine differences in bacterial abundance, individual t tests were conducted between the control group (H₂O-Sal) and every other group. All t tests were two-tailed. SCFA levels in caecum were converted to fold change and significance was determined using a 3×2 mixed ANOVA with metabolite as a fixed within-subjects factor and drink type as a fixed between-subjects factor. Locomotor sensitization over days was analyzed using a 5×2 mixed ANOVA with day as a fixed within-subject factor and drink type as a fixed between-subject factor. Persistence of sensitization was analyzed using an independent samples t test. For morphine place preference with two conditioning days (2.5–10 mg/kg), preference score was analyzed using a 3×2 between-subjects ANOVA with morphine dose and drink type as fixed factors. For three conditioning days (15 mg/kg), the two groups were compared using an independent samples t test. For validation of reversal of Abx effects on CPP after SCFA replenishment, data was analyzed using a one or two-way ANOVA as appropriate with Fisher's LSD test for planned pairwise comparisons to the H₂O control group. Statistical significance for qPCR was determined using separate 2×2 between-subjects ANOVAs for each target, with Abx (presence or absence) and SCFA (presence or absence) as fixed factors and Tukey's HSD was applied in the presence of a significant interaction. Unless otherwise stated, p values < 0.05 were deemed statistically significant.

RESULTS

Oral Abx reduces microbiome diversity and alters the proportion of dominant bacterial populations in control and morphine-treated mice

Similar to our previous work [18], we used nonabsorbable broad-spectrum antibiotics to induce a robust microbiome knockdown. This allows for interrogation of the effect of a deficient microbiome in a normally developed mouse [46]. Mice were given 2 weeks of oral Abx delivered in their drinking water starting at 8 weeks of age before the start of once daily morphine injections (20 mg/kg, s.c.) for 7 days (Fig. 1A). This yielded four treatment groups: H₂O-Sal, Abx-Sal, H₂O-Mor, and Abx-Mor. As observed previously [18], chronic Abx did not cause deleterious effects on animal health. Abx mice exhibited the same amount of weight gain (Supplementary Fig. 1). Abx also did not affect morphine metabolism or brain penetrance (Supplementary Fig. 2).

However, as expected, Abx treatment significantly reduced alpha diversity as measured by the number of unique observed taxonomic units (OTUs, Fig. 1B—main effect of Abx: $F_{(1, 14)} = 116.5$, $p < 0.0001$; no effect of morphine: $F_{(1, 14)} = 2.14$, $p = 0.17$ and no interaction: $F_{(1, 14)} = 0.14$, $p = 0.72$) and by the Shannon diversity index (Fig. 1C—main effect of Abx: $F_{(1, 14)} = 286.4$, $p < 0.0001$; no effect of morphine: $F_{(1, 14)} = 2.82$, $p = 0.12$ and no interaction: $F_{(1, 14)} = 0.01$, $p = 0.91$). Planned pairwise comparisons identified significant pairwise comparisons between H₂O-Sal and Abx-Sal, H₂O-Sal and Abx-Mor, and between H₂O-Morphine and Abx-Mor (all $p < 0.0001$) for both measures.

However, morphine itself had minimal effects on microbiome composition, in contrast to other reports [36, 47–49]. There was no difference between H₂O-Sal and H₂O-Mor on measures of alpha diversity (observed OTUs: $t_{(14)} = 0.73$, $p = 0.47$ and Shannon index: $t_{(14)} = 1.21$, $p = 0.25$). Beta diversity assessed using an unweighted UniFrac dissimilarity matrix shows near complete overlap between samples in H₂O-Sal and H₂O-Mor groups (Fig. 1D) and relative proportions of bacterial phyla were similar between H₂O-Sal and H₂O-Mor (Fig. 1E). Only two of the top ten most abundant phyla were significantly reduced by morphine alone: Rokubacteria ($t_{(7)} = 8.08$, $p < 0.0001$) and Cyanobacteria ($t_{(7)} = 3.65$, $p = 0.0082$); however, these phyla are expressed at very low abundance in all tested groups (both $< 0.1\%$, Fig. 1F).

Abx, whether alone or in combination with morphine, also had a substantial effect on microbial composition as well as diversity. Both Abx-Sal and Abx-Mor groups had significant shifts in relative proportions of 7/10 major phyla, with the largest effects being a drastic reduction in Firmicutes (Abx-Sal: $t_{(7)} = 26.12$, $p < 0.0001$; Abx-Mor: $t_{(7)} = 12.39$, $p < 0.0001$) and expansion of both Bacteroidetes (Abx-Sal: $t_{(7)} = 16.32$, $p < 0.0001$, Abx-Mor: $t_{(7)} = 10.27$, $p < 0.0001$) and Verrucomicrobia (Abx-Sal: $t_{(7)} = 6.39$, $p = 0.0004$, Abx-Mor: $t_{(7)} = 8.43$, $p < 0.0001$), Fig. 1F.

Interestingly, the combination of Abx and morphine induced shifts in the microbiome that were different from both Abx-Sal and H₂O-Mor. Abx-Sal and Abx-Mor are more similar to each other than the H₂O groups based on phyla abundance (Fig. 1E), but sample clustering by Unifrac distance suggest these samples are from distinct populations (Fig. 1D). At the level of individual phyla, Actinobacteria was significantly changed in Abx-Mor only (Abx-Sal: $t_{(7)} = 0.22$, $p = 0.83$; Abx-Mor: $t_{(7)} = 5.11$, $p = 0.0014$) and Abx-Mor caused a reduction in the proportion of Proteobacteria ($t_{(7)} = 3.40$, $p = 0.011$) while Abx-Sal caused a significant increase ($t_{(7)} = 2.55$, $p = 0.038$, Fig. 1F). All fold change, p values, and mean % abundance are included in Supplementary Table 1.

Bacterial enzymes that synthesize SCFA are predicted to be downregulated in Abx-Mor mice and SCFA levels are reduced in Abx-treated mice

Given the decrease in overall bacterial abundance found in Abx groups, we next focused on predicted functional enzymatic pathways that might be differentially affected by Abx and morphine. Phyla-level analysis indicated that there was a drastic reduction in the proportion of Firmicutes in Abx groups compared to control (Fig. 1F); many bacterial species in this phylum are producers of the SCFA butyrate [50, 51]. We identified enzymes that are predicted to be involved in butyrate and propionate synthesis using Phylogenetic Investigation of Communities by Reconstruction of Unobserved States (PICRUSt2) [52]. Direct comparison of mean sequence proportion between Abx-Mor and H₂O-Sal mice predicted multiple differentially regulated enzymes in Abx-Mor related to butyrate synthesis (Supplementary Fig. 3A) and propionate synthesis (Supplementary Fig. 3B) [50]. Full PICRUSt2 list is supplied as Supplementary Table 2.

To confirm the predicted results from PICRUSt2, levels of the three most abundant SCFA—acetate, butyrate, and propionate—were quantified in the caecal contents of a separate group of Abx-treated mice. Indeed, Abx significantly decreased levels of SCFA in

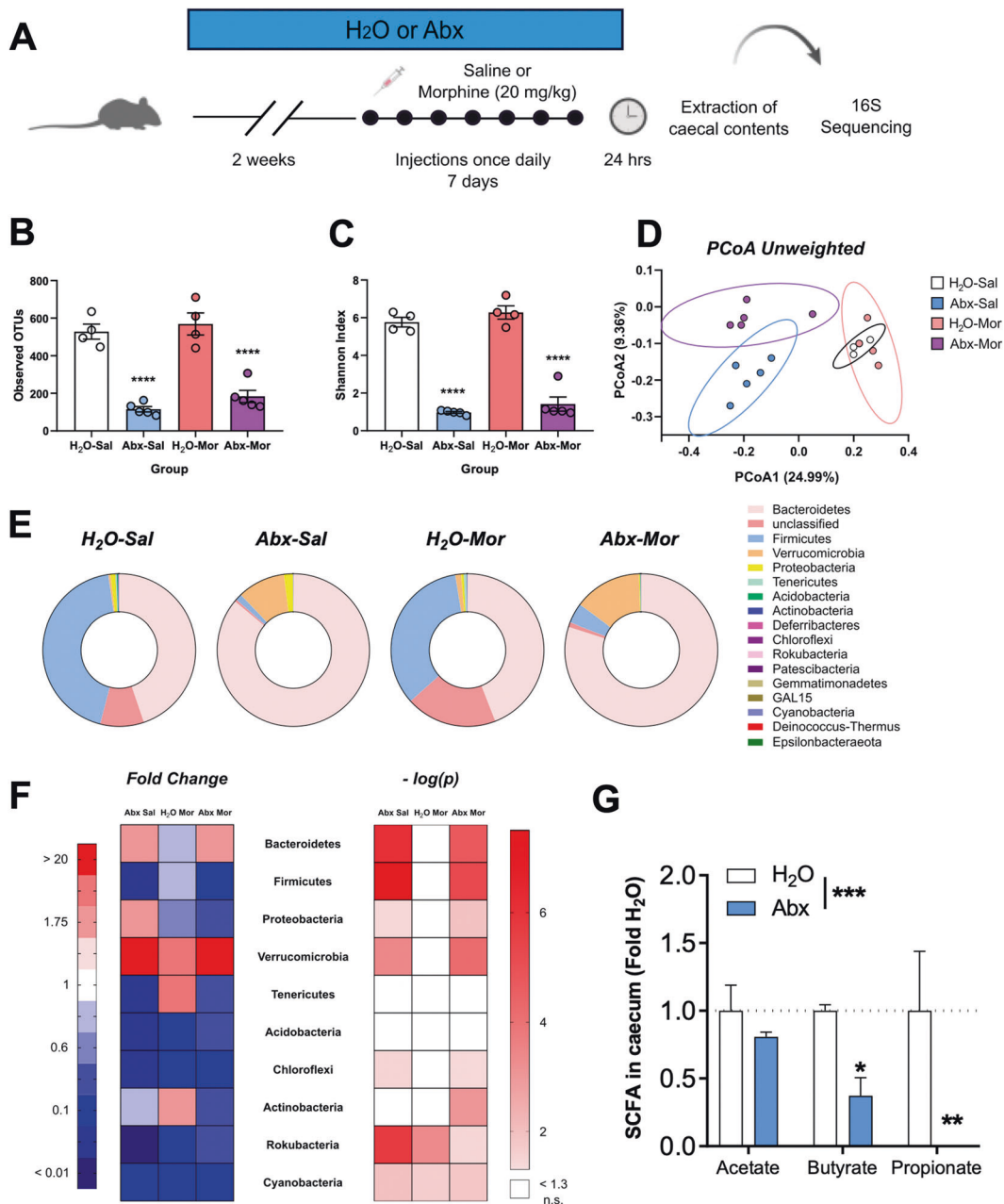


Fig. 1 Oral Abx alters the microbiome. **A** Experimental timeline. **B**, **C** Abx reduces alpha diversity as measured by observed OTUs and the Shannon index. **D** Mice from Abx-Sal and Abx-Mor possess unique microbiomes, but H₂O-Sal and H₂O-Mor populations overlap as measured using the unweighted UniFrac distance. **E** Relative phylum abundance in all groups of mice, each phylum shown in a different color. **F** Heatmap displaying the fold change (left) and $-\log(p)$ value (right) of the top ten most abundant phyla in control mice. Fold change values in red have greater abundance in that group compared to H₂O-Sal and blue values have less abundance (left). Negative log(p) values in pink or red are significant (right). **G** Abx reduces levels of the caecal SCFA. Data shown as fold change from H₂O treated mice. Data presented as means \pm SEM. * p < 0.05; ** p < 0.01; **** p < 0.0001.

caecal content (main effect of drink type: $F_{(1, 8)} = 29.41$, $p = 0.0006$; no effect of metabolite: $F_{(2, 16)} = 1.54$, $p = 0.24$ and no interaction: $F_{(2, 16)} = 1.54$, $p = 0.24$). Planned comparisons between H₂O and Abx mice found that butyrate ($t_{(24)} = 2.18$, $p = 0.039$) and propionate ($t_{(24)} = 3.47$, $p = 0.002$), but not acetate ($t_{(24)} = 0.67$, $p = 0.51$) were significantly reduced by Abx (Fig. 1G).

Microbiome depletion reduces morphine locomotor sensitization and morphine reward

To determine the behavioral effects of microbiome knockdown, mice were tested for morphine locomotor sensitization and

morphine CPP. Both H₂O and Abx mice developed locomotor sensitization to repeated morphine (main effect of day: $F_{(2,81, 22,50)} = 7.83$, $p = 0.0011$), but there was no effect of Abx ($F_{(1, 8)} = 0.79$, $p = 0.40$) and no interaction between day and Abx ($F_{(4, 32)} = 1.45$, $p = 0.24$), Fig. 2A. Upon morphine challenge given 10 days later, Abx mice had reduced persistence of locomotor sensitization compared to H₂O mice ($t_{(8)} = 2.73$, $p = 0.026$, Fig. 2B).

Locomotor sensitization is often used as a tool for drug-induced neural plasticity, but it has little specificity as a model of reward. To better assess whether microbiome knockdown could influence opioid reward, mice from H₂O and Abx cages were trained on

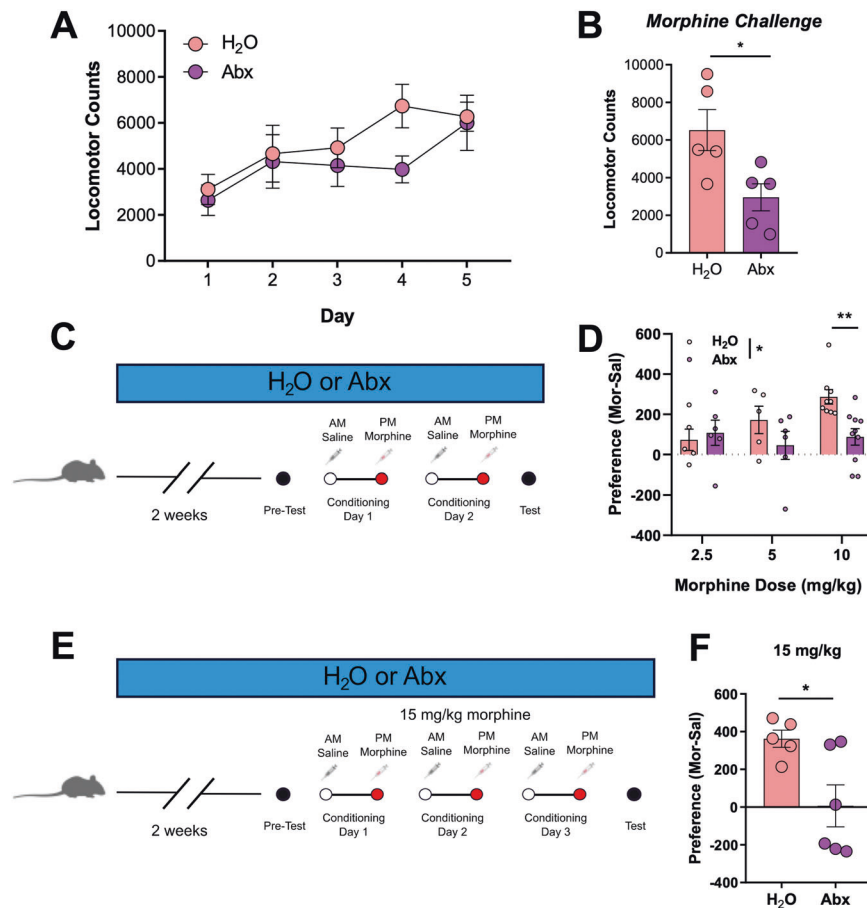


Fig. 2 Microbiome knockdown reduces locomotor sensitization and morphine place preference. **A** Abx did not alter the locomotor response to repeated morphine but did reduce sensitization (**B**). **C** Experimental timeline for 2-pairing CPP. **D** Abx treatment reduced high-dose morphine CPP. **E** Experimental timeline for 3-pairing CPP. **F** Abx mice did not demonstrate morphine CPP with three morphine-chamber pairings at a high dose (15 mg/kg). Data presented as means \pm SEM. * $p < 0.05$.

morphine CPP. CPP occurred over 4 days with 2 days of conditioning (Fig. 2C). On conditioning days, all mice were given injections of saline in the morning and 2.5, 5, or 10 mg/kg morphine in the afternoon. Microbiome knockdown reduced morphine place preference (main effect of drink type: $F_{(1, 35)} = 4.76$, $p = 0.036$; no effect of dose: $F_{(2, 35)} = 2.13$, $p = 0.13$ and no interaction: $F_{(2, 35)} = 2.55$, $p = 0.09$). Pairwise comparisons demonstrated that Abx mice specifically had reduced preference for the morphine-paired chamber at the 10 mg/kg dose ($t_{(35)} = 3.17$, $p = 0.003$), Fig. 2D.

To fully account for potential effects on dose response and changes in associative learning, we then performed enhanced morphine CPP conditioning with both an additional conditioning day (3 days vs. 2 days) and a higher dose of morphine (15 mg/kg, Fig. 2E). Similar to their response at 10 mg/kg morphine, Abx mice had a reduced CPP score compared to H₂O mice ($t_{(9)} = 2.74$; $p = 0.023$), Fig. 2F. Interestingly, the magnitude of effect increased as the dose of morphine increased (Cohen's d 2.5 mg/kg = 0.26; 5 mg/kg = 0.78, 10 mg/kg = 1.04; 15 mg/kg = 1.73), suggesting that Abx more efficiently reduces the effects of high-dose opioids and this effect is unlikely due to impaired learning alone, since more morphine pairings potentiated the effect.

Microbiome knockdown alters the NAC transcriptional response to morphine

While many brain areas contribute to drug reward and the development of addiction, the NAC is heavily implicated in primary reward. Lesions of this region abolish place preference

and reduce ongoing self-administration [53, 54], making it an attractive neurobiological target to investigate molecular effects involved in the attenuation of morphine reward caused by microbiome knockdown. To explore the impact of microbiome depletion on gene expression in the NAc, H₂O, and Abx mice were given seven daily injections of saline or morphine (20 mg/kg, s.c.) followed by NAc collection 24 h after their last injection (Fig. 3A). RNA-sequencing revealed minor gene expression differences in mice receiving Abx alone compared to controls, with 51 transcripts differentially regulated in the Abx-Sal group (Fig. 3B). In contrast, there were 946 differentially regulated in the H₂O-Mor group with the majority being increased in expression (Fig. 3C). However, the combination of Abx and morphine produced substantial gene expression differences that were greater than the effects of morphine and Abx alone, with 2806 genes downregulated and 2689 genes upregulated compared to controls (Fig. 3D). For full list of all significantly regulated genes in all comparisons, see Supplementary Table 3.

To better understand how specific gene pathways were altered by morphine treatment in mice with and without a normal microbiome, we next performed Gene-Ontology (GO) pathway analysis on significantly regulated genes from these three groups. We see that while morphine treatment regulated similar pathways in mice with and without a gut microbiome, the magnitude of the pathway effect was often greater in the Abx-Mor treated mice (Fig. 3E). Notably, Abx-Sal pathways are not depicted on the graph as none of these pathways had a

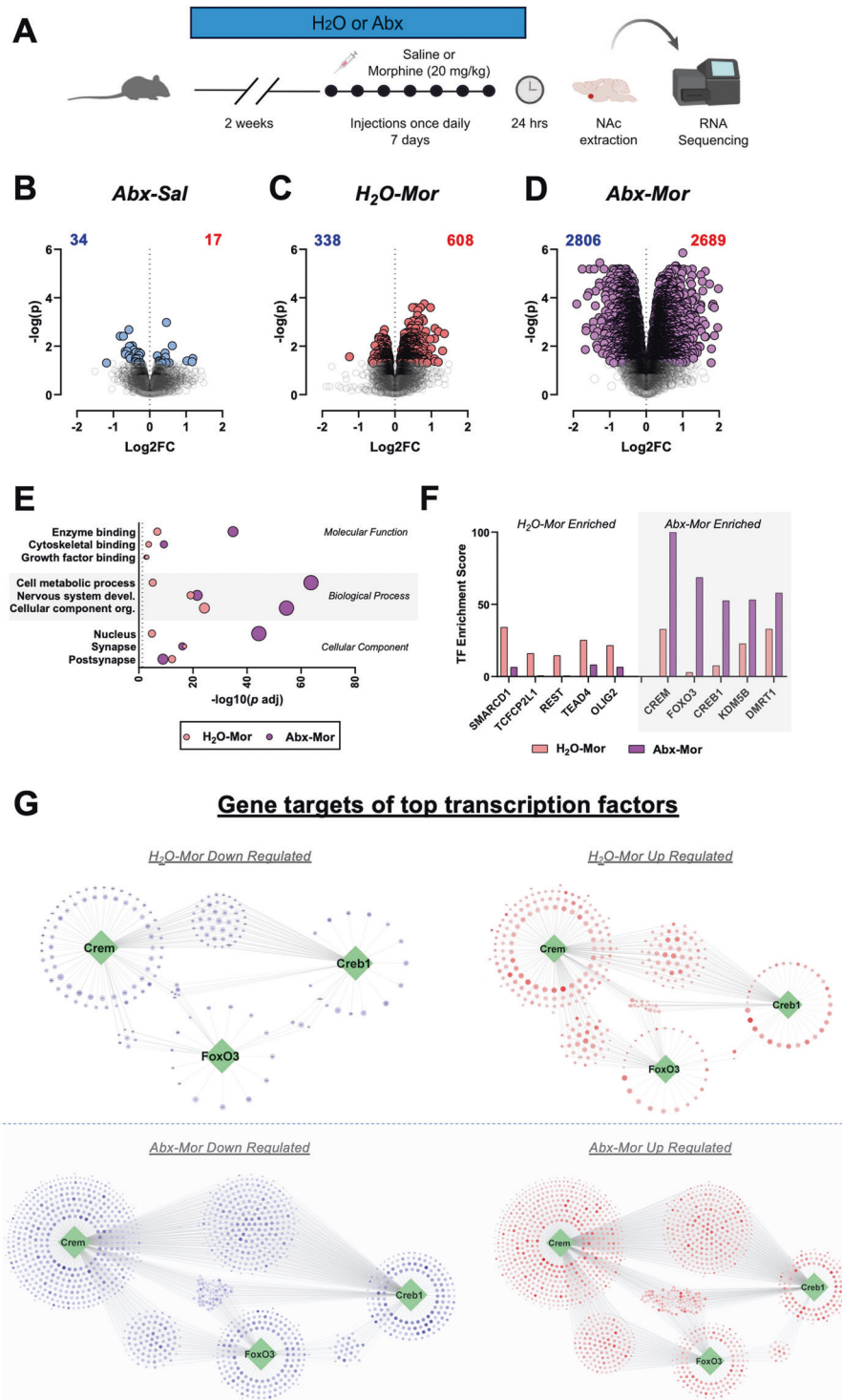


Fig. 3 Morphine and Abx alter the NAc transcriptome. **A** Experimental timeline for RNA-sequencing. **B–D** Volcano plots depicting differential gene expression between H₂O-Sal and Abx-Sal (**B**), H₂O-Mor (**C**), and Abx-Mor (**D**). Colored circles are significantly differentially regulated transcripts identified using an FDR corrected $p < 0.05$. **E** Representation of some top gene-ontology terms regulated in morphine groups. The x-axis is the FDR-corrected $-\log(p)$ value with the dotted line indicating a FDR corrected $p < 0.05$, and circle size represents number of genes per term. **F** Top differentially predicted transcription factors using Chea software analysis demonstrates factors with different predicted effects between groups. Y-axis is the overall transcription factor enrichment score predicted from genes in the dataset. **G** Cloud diagrams depicting top regulated transcription factors (hubs) and their predicted downstream targets (nodes).

$-\log(p) > 1.3$ (i.e., not statistically significant) and thus would not show up on the graph. Abx-Mor mice had particular enrichment in pathways related to enzyme binding, cellular metabolism, and nuclear localization. However, H₂O-Mor mice had more

significant regulation of growth factor binding and postsynapse related genes, suggesting functional differences in how the two groups respond to the drug. Full pathway lists available for all comparisons in Supplementary Table 4.

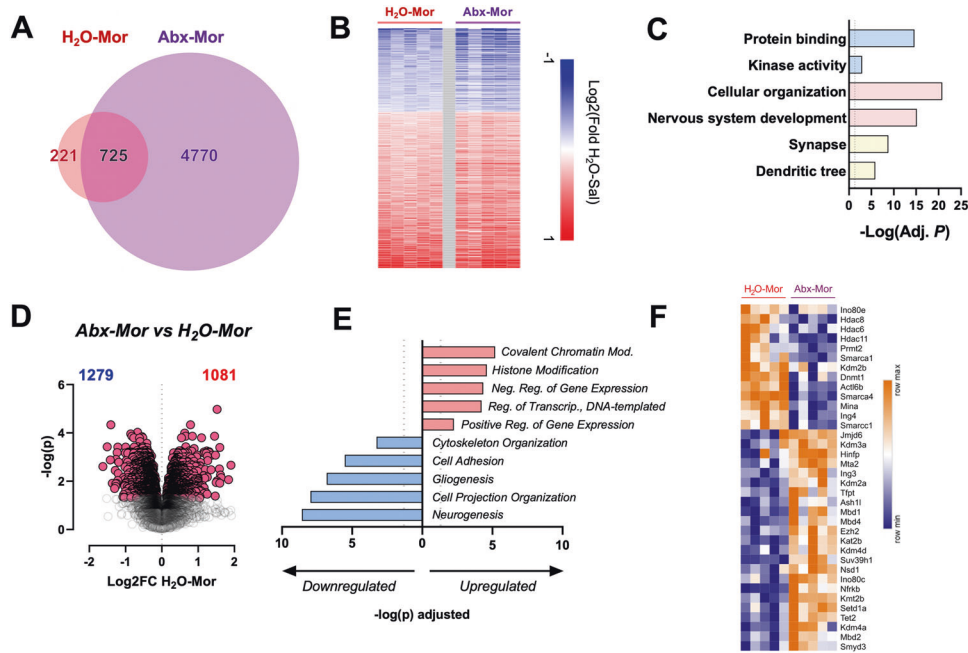


Fig. 4 Microbiome knockdown alters the NAc transcriptional response to morphine. **A** Venn diagram depicting number of differentially regulated genes of H₂O-Mor vs. H₂O-Sal (pink) and Abx-Mor vs. H₂O-Sal (purple). **B** Heatmap of genes that are differentially regulated by both H₂O-Mor and Abx-Mor. **C** Gene-ontology pathway analysis of overlapping genes. **D** Volcano plots depicting differential gene expression between Abx-Mor and H₂O-Mor. Colored circles are significantly differentially regulated transcripts identified using an FDR $p < 0.05$. **E** Gene-ontology pathways up and downregulated between Abx-Mor and H₂O-Mor. Pink pathways are upregulated, and blue pathways are downregulated. Dotted vertical line is the significance cut-off of FDR $p < 0.05$. **F** Heatmap depicting all significantly regulated histone modifiers between Abx-Mor and H₂O-Mor.

Given the extent of the transcriptional changes between the two groups, we also sought to determine how changes in transcription factor activity might be playing a role in gene regulation in this model. Using data from the ChEA transcription factor dataset, which utilizes ChIP-seq datasets to identify transcription factor binding peaks in the promoters of genes [55] along with the Enrichr software package [56, 57], we identified transcription factors with the greatest differential transcription factor enrichment score between the H₂O-Mor and Abx-Mor groups (Fig. 3F). We see that relative to genes in Abx-Mor mice, H₂O-Mor mice had regulation of genes known to be bound by SMARCD1, TCF21, and REST; whereas the top relative transcription factors predicted in Abx-Mor mice relative to H₂O-Mor were CREM, FOXO3, and CREB1. Full data on transcription factor binding enrichment predicted via Enrichr are available as Supplementary Table 5. To better visualize the differences in predicted transcription factor activation patterns we performed analysis looking at up and downregulated genes downstream from the three transcription factors most enriched in the Abx-Mor group. As can be seen in Fig. 3G these transcription factors regulate networks of highly overlapping genes. However, in the H₂O-Mor groups there are more distinct patterns of downstream genes that are primarily upregulated rather than downregulated. Whereas antibiotic treated mice show widespread up and downregulation of genes downstream from these factors—portending a much more widespread transcriptional dysregulation of these pathways in mice lacking a complex microbiome.

Given the differential behavioral response to morphine in mice with a depleted microbiome, we next investigated how microbiome depletion specifically affected the transcriptional response to morphine. When examining genes differentially regulated relative to H₂O-Sal we see that there is considerable overlap between genes affected in the H₂O-Mor and Abx-Mor groups (Fig. 4A, data visualized using BioVenn [58]), with ~77% of those genes regulated by morphine in the H₂O group also being

regulated in the Abx group. Further, when the direction of change was analyzed, we see that nearly all of these genes that were changed by morphine in both treatment groups were changed in the same direction (Fig. 4B). GO pathway analysis shows that genes similarly affected by morphine in both Abx and H₂O groups had functionality related to protein binding, cellular organization, and synapse-related genes among others (Fig. 4C) full pathway analysis on overlapping genes available as Supplementary Table 6).

To further investigate how the microbiome alters responses to morphine, we performed transcriptomic analysis comparing the two morphine-treated groups. In direct comparison, Abx-Mor caused differential expression of 2360 genes (1279 downregulated, 1081 upregulated) when compared to H₂O-Mor (Fig. 4D). Pathway analysis on genes differentially regulated between H₂O-Mor and Abx-Mor identified several pathways related to epigenetic modification that were upregulated in the Abx-Mor group, including covalent chromatin modification, histone modification, negative regulation of gene expression, and positive regulation of gene expression (Fig. 4E). Downregulated pathways were more varied but included neurogenesis, cell projection organization, gliogenesis, and cytoskeleton organization (for full list of significantly regulated pathways, see Supplementary Table 4). To visualize the effect of Abx-Mor on the expression of histone modifiers, the Database of Epigenetic Modifiers (dBEM) [59], a curated list of human epigenetic modifiers from healthy and cancerous genomes, was used to identify epigenetic regulators in the dataset (Fig. 4F), demonstrating that Abx differentially influences epigenetic modifier expression after morphine.

Replenishment of SCFA reverses gene expression changes and morphine reward deficit caused by Abx
Since knockdown of the microbiome altered the behavioral (Fig. 2) and transcriptional responses (Figs. 4, 5) to morphine in line with a

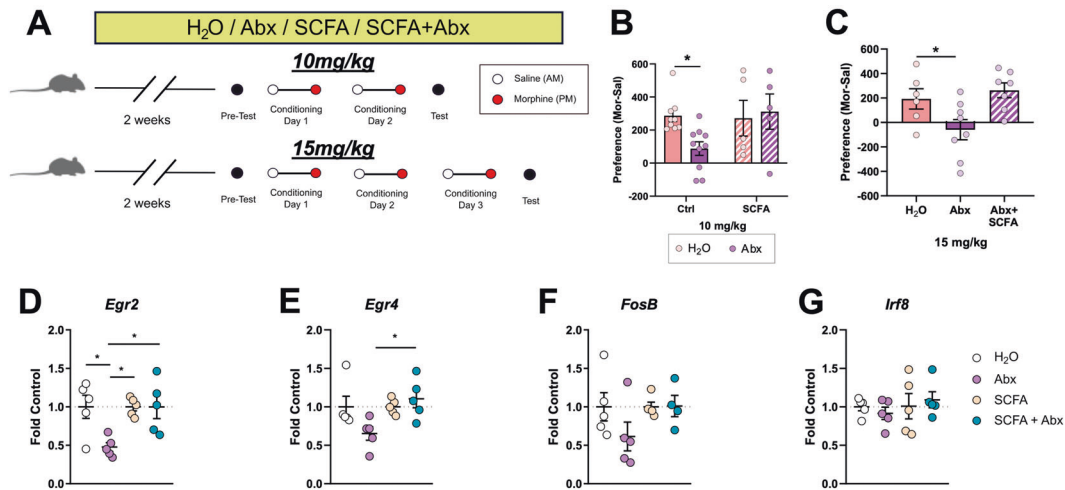


Fig. 5 Replenishment of SCFAs reverses reward deficit and gene expression changes caused by microbiome depletion. **A** Experimental timeline for CPP after SCFA replenishment. SCFA supplementation restored morphine place preference in Abx-treated mice when trained at 10 mg/kg morphine with 2 conditioning days (**B**) or at 15 mg/kg morphine with 3 conditioning days (**C**). SCFA + Abx normalized gene expression for *Egr2* (**D**) and *Egr4* (**E**) but did not change expression of *FosB* (**F**) or *Irf8* (**G**). Data are presented as mean ± SEM. **p* < 0.05.

reduction in SCFA signaling (Fig. 1G), we next examined if repletion of the SCFA via the drinking water could reverse the effects of microbiome depletion. For these purposes, mice received treatment with H₂O, Abx, a cocktail of SCFA known to recapitulate physiological levels of SCFA [14, 18, 60], or combination SCFA + Abx before examination of their effects on morphine CPP. Mice underwent the 2-day conditioning protocol using 10 mg/kg morphine (Fig. 5A). Two-way ANOVA found no significant main effects (Fig. 5B—Abx: $F_{(1, 25)} = 1.48, p = 0.23$; SCFA: $F_{(1, 25)} = 2.53, p = 0.12$) with a trend toward significant interaction ($F_{(1, 25)} = 3.33, p = 0.08$). However, pairwise comparisons indicated that Abx reduced morphine place preference when compared to H₂O as shown previously ($t_{(25)} = 2.59, p = 0.016$) and SCFA did not influence place preference by itself (SCFA vs. H₂O: $t_{(25)} = 0.16, p = 0.87$). However, SCFA supplemented mice with a reduced microbiome demonstrated normal morphine place preference (SCFA + Abx vs. H₂O: $t_{(25)} = 0.26, p = 0.80$). This critical finding shows that the presence of SCFA metabolites can regulate behavior, even in the absence of a complex microbiome. To further validate this behavioral reversal of microbiome depletion by SCFA we also performed CPP at the high dose of cocaine with 3 conditioning sessions where we saw the largest effect of microbiome depletion (as in Fig. 2F). Here, we again see that Abx treatment leads to a marked reduction of morphine CPP (main effect of drink type $F_{(2, 18)} = 5.24, p = 0.016$; H₂O compared to Abx $t_{(18)} = 2.11, p = 0.03$), but repletion of the SCFA metabolites in mice with a depleted microbiome reverses the effects of Abx (H₂O compared to Abx + SCFA $t_{(11)} = 0.6, p = 0.53$, Fig. 5C).

Using the same Abx and SCFA repletion paradigm, we then performed quantitative PCR analysis of gene expression levels in the NAc focused on targets known to be affected in the Abx-Mor groups from above (primers used for transcript quantification are available as Supplementary Table 7). Here we found significant effects of drink type on multiple transcription factors including *Egr2* (main effect of Abx: $F_{(1, 16)} = 5.27, p = 0.036$, main effect of SCFA: $F_{(1, 16)} = 5.23, p = 0.036$, and a significant interaction $F_{(1, 16)} = 5.23, p = 0.036$, Fig. 5D) and *Egr4* (main effect of SCFA: $F_{(1, 16)} = 4.87, p < 0.042$ and a significant interaction: $F_{(1, 16)} = 4.87, p < 0.42$, Fig. 5E; no effect of Abx: $F_{(1, 16)} = 1.43, p = 0.25$), but no effect on transcript levels of *FosB* (Abx: $F_{(1, 16)} = 0.80, p = 0.39$; SCFA: $F_{(1, 16)} = 2.64, p = 0.12$; interaction: $F_{(1, 16)} = 2.64, p = 0.12$, Fig. 5F) or *Irf8* (Abx: $F_{(1, 16)} = 0.0001, p = 0.992$; SCFA: $F_{(1, 16)} = 0.72, p = 0.41$; interaction: $F_{(1, 16)} = 0.61, p = 0.45$, Fig. 5G). Importantly, SCFA + Abx affected transcription of both *Egr2* and *Egr4*

differently than Abx alone; Tukey's post hoc analysis indicated that Abx alone reduced *Egr2* compared to H₂O ($p = 0.024$), but there was no difference in *Egr2* expression between SCFA and SCFA + Abx ($p > 0.9999$, Fig. 5D). Additionally, Abx decreased expression of *Egr4* (non-significant, trending); but levels of *Egr4* were significantly increased in response to SCFA + Abx compared to Abx alone ($p = 0.03$, Fig. 5E). This indicates that, despite a reduction in microbial diversity via Abx, supplementation of SCFA back into drinking H₂O can reverse expression patterns of several different transcription factors and suggests a mechanism for transcriptional effects seen in our full RNA-seq dataset.

DISCUSSION

The current set of studies demonstrate that a complete and complex microbiome produces metabolites (SCFA) that are necessary for morphine reward using a CPP model. Oral Abx successfully reduced the complexity of the gut microbiome (Fig. 1B, C) and reduced caecal SCFA content (Fig. 1G) but had no observed off-target health effects (Supplementary Figs. 1, 2). Using this model, we saw that knockdown of the microbiome attenuated morphine place preference (Fig. 2D, F) and locomotor sensitization (Fig. 2B). While perturbations to the microbiome affect multiple physiological functions, our data suggest that the reduction in SCFA (Fig. 1G) due to microbiome knockdown drives the behavioral effects of Abx, since replenishment of SCFA to Abx-treated mice restored morphine CPP (Fig. 5B, C) and led to a partial reversal of Abx-induced transcriptional changes (Fig. 5D–G).

The SCFA are metabolic byproducts of the bacterial fermentation of insoluble fiber, and they have multiple cellular mechanisms [34]. Importantly, there are multiple paths by which SCFAs can affect gene expression. They are known to alter transcription factor activity including CREB [27–30], they alter the activity of chromatin modifying enzymes including histone deacetylases [24, 61–63], and can even serve as carbon sources for histone acylations [25, 26]—any one of which can have marked effects on chromatin structure and gene expression. Given the marked changes in behavioral and transcriptional response to morphine in microbiome-depleted mice and the ability of SCFA repletion to reverse these effects, we propose a model wherein a complex gut microbiome and its metabolites serve as a homeostatic regulator of experience dependent gene transcription in the brain. When the microbiome is depleted, robust external stimuli such as repeated exposure to drugs of abuse leads to dramatic changes in behavioral and

transcriptional response. When gut metabolites such as the SCFA are returned, this homeostatic mechanism is restored and response to drugs of abuse or other external stimuli is restored.

These are certainly not the first findings to demonstrate that changes in the microbiome can affect transcriptional control in the brain. Interestingly, mice raised fully germ-free have altered expression at baseline of immediate early genes and other activity induced genes in the amygdala and prefrontal cortex, with more robust changes in gene expression occurring in response to an external stimulus [17, 64]. Another recent paper that also utilized antibiotic depletion found robust changes in gene expression in response to reactivation of a fearful stimulus [16]. Interestingly, this same paper used single nucleus sequencing to demonstrate that knockdown of microbiome complexity leads to changes in gene expression in all cell types identified [16]. Other papers that have looked at sorted microglia have found that germ-free or antibiotic treated mice have robust changes to microglial gene expression and chromatin structure [14, 15]. Future studies in our model of substance use disorder will seek to investigate cell-specific effects to tease apart the full mechanism underlying microbiome–morphine interactions.

CPP is a useful tool for assessing a drug's rewarding value and requires an animal to associate a distinct environment with a drug's effects [65]. Place preference can only occur if an animal successfully learns the environment–drug association and simultaneously finds that drug rewarding. In the current study, it is not clear whether the Abx-induced reduction in morphine CPP was due to a decrease in the subjective rewarding properties of morphine or an impairment in environment–drug association. In general, HDACs act to repress gene expression and tend to inhibit learning processes and HDAC inhibitors such as SCFA strengthen them [66]. Previous work has demonstrated enhanced morphine reward and sensitization after systemic sodium butyrate injections in microbiome-intact mice [67] and a study showed potentiated heroin place preference after NAC HDAC inhibition [68]. In our antibiotic depletion model mice have reduced levels of butyrate and other SCFAs (Fig. 1G), and show decreased CPP (Fig. 2D, F) which suggests that these molecular pathways are key for formation of CPP. Interestingly, our control mice who received oral SCFA with a regular microbiome (Fig. 5B) did not show any change in preference. This may be due to route and timing of administration. Previous work utilized higher dose butyrate (120 mg/kg) that was injected prior to drug treatment [67] whereas our mice were orally consuming 40 mM butyrate overnight in the home cage. These differences in findings raise important questions about kinetics and molecular mechanisms that will be the subject of future studies.

Previous work on the microbiome and opioids has shown that depletion of the gut microbiome, or germ-free status, reduces the formation of opioid tolerance [36, 37]. While our regimen of morphine does not produce any symptoms of physical dependence or withdrawal, when considering the translational implications of gut–brain interactions in OUD, these studies are an important parallel to ours. Given that morphine tolerance and opioid-induced hyperalgesia can be key drivers of pathological opioid use, the fact that the microbiome can alter both opioid tolerance and reward is a key component to understanding how gut–brain interactions can be targeted to reduce the burden of OUD in human subjects.

Interestingly, while our studies showed marked effects of microbiome depletion on brain and behavior, we saw no effects of morphine treatment on microbiome composition. This is interesting as several other studies have shown family and species level changes in microbiome composition following prolonged morphine [36, 47–49]. While morphine has known effects on gastrointestinal motility and function, it is noteworthy that in these studies when morphine induced microbiome changes were seen the drug regimen used was one designed to elicit morphine

tolerance or physical dependence with consistently infused morphine via implanted pellet [47–49], or daily escalating doses [36, 49]. While we have not specifically assessed tolerance or withdrawal in our mice, we do not observe signs consistent with opioid withdrawal even in our high-dose mice. It is possible that the induction of tolerance leads to more marked changes in gastrointestinal motility or otherwise affects the intestinal milieu to more markedly affect microbiome composition. Based on this, it seems highly likely that opioid-induced changes in microbiome composition are dependent on interactions of timing, dose, and route of administration, and further work will be required to clarify the specific interactions.

The current paper demonstrates that the gut microbiome and its metabolites, the SCFA, are crucial mediators of morphine reward. Reduction of the microbiome attenuated morphine place preference, and this effect was reversed by repletion of SCFA. These studies also point to altered transcriptional control within the NAc as a potential mechanism linking the microbiome to morphine reward. Understanding how peripheral systems such as the gut microbiome interact with the brain to affect drug reward is an exciting avenue of research; these studies could aid in the development of safe mitigation strategies to be used in conjunction with maintenance therapy in the treatment of OUD.

FUNDING AND DISCLOSURE

This work was supported by NIDA grants DA044308, DA049568, and DA051551 to DDK and DA050906 to RSH as well as by NARSAD Young Investigator Awards to RSH and DDK. The authors declare no competing interests.

DATA AVAILABILITY

All RNA-sequencing files will be uploaded to the publicly available Gene Expression Omnibus server and will be linked to this publication. All data in this paper will be made available upon reasonable request.

ACKNOWLEDGEMENTS

Morphine sulfate was provided by the NIDA Drug Supply Program. We acknowledge the Microbial Culture & Metabolomics Core of the PennCHOP Microbiome Program for performing targeted metabolomics analyses. Parts of Figs. 1, 2, 3, and 5 were created with Biorender.com with full permission to publish.

AUTHOR CONTRIBUTIONS

DDK and RSH designed the experiments. RSH, NLM, TJE, KRM, ATO, and DDK performed experiments. RSH, TJE, KRM, ATO, and DDK analyzed data. RSH and DDK wrote the paper. All authors provided critical edits and feedback of the finalized paper.

ADDITIONAL INFORMATION

Supplementary information The online version contains supplementary material available at <https://doi.org/10.1038/s41386-021-01043-0>.

Publisher's note Springer Nature remains neutral with regard to jurisdictional claims in published maps and institutional affiliations.

REFERENCES

1. Substance Abuse and Mental Health Services Administration. The NSDUH report. Rockville, Md.: Office of Applied Studies, Substance Abuse and Mental Health Services Administration, Dept. of Health & Human Services; 2008.
2. Hedegaard H, Miniño AM, Warner M. Drug Overdose Deaths in the United States, 1999–2018. NCHS Data Brief. 2020;356:1–8.
3. Schuckit MA. Treatment of opioid-use disorders. N Engl J Med. 2016;375:357–68.
4. Evans CJ, Cahill CM. Neurobiology of opioid dependence in creating addiction vulnerability. F1000Research. 2016;5:F1000 Faculty Rev-1748.
5. Chopra N, Marasa LH. The opioid epidemic: challenges of sustained remission. Int J Psychiatry Med. 2017;52:196–201.

6. Rea K, Dinan TG, Cryan JF. Gut microbiota: a perspective for psychiatrists. *Neuropsychobiology*. 2020;79:50–62.
7. Meckel KR, Kiraly DD. A potential role for the gut microbiome in substance use disorders. *Psychopharmacology*. 2019;236:1513–30.
8. Adams JB, Johansen LJ, Powell LD, Quig D, Rubin RA. Gastrointestinal flora and gastrointestinal status in children with autism—comparisons to typical children and correlation with autism severity. *BMC Gastroenterol*. 2011;11:22.
9. Cheung SG, Goldenthal AR, Uhlemann A-C, Mann JJ, Miller JM, Sublette ME. Systematic review of gut microbiota and major depression. *Front Psychiatry*. 2019;10:34.
10. Cryan JF, O’Riordan KJ, Sandhu K, Peterson V, Dinan TG. The gut microbiome in neurological disorders. *Lancet Neurol*. 2020;19:179–94.
11. Cenit MC, Sanz Y, Codoñer-Franch P. Influence of gut microbiota on neuropsychiatric disorders. *World J Gastroenterol*. 2017;23:5486–98.
12. Foster JA, Rinaman L, Cryan JF. Stress & the gut-brain axis: regulation by the microbiome. *Neurobiol Stress*. 2017;7:124–36.
13. Bravo JA, Forsythe P, Chew MV, Escaravage E, Savignac HM, Dinan TG, et al. Ingestion of *Lactobacillus* strain regulates emotional behavior and central GABA receptor expression in a mouse via the vagus nerve. *Proc Natl Acad Sci USA*. 2011;108:16050–5.
14. Erny D, Hrabě de Angelis AL, Jaitin D, Wieghofer P, Staszewski O, David E, et al. Host microbiota constantly control maturation and function of microglia in the CNS. *Nat Neurosci*. 2015;18:965.
15. Thion MS, Low D, Silvin A, Chen J, Grisel P, Schulte-Schrepping J, et al. Microbiome influences prenatal and adult microglia in a sex-specific manner. *Cell*. 2018;172:500–16.e16.
16. Chu C, Murdock MH, Jing D, Won TH, Chung H, Kressel AM, et al. The microbiota regulate neuronal function and fear extinction learning. *Nature*. 2019;574:543–8.
17. Hoban AE, Stilling RM, Ryan FJ, Shanahan F, Dinan TG, Claesson MJ, et al. Regulation of prefrontal cortex myelination by the microbiota. *Transl Psychiatry*. 2016;6:e774.
18. Kiraly DD, Walker DM, Calipari ES, Labonte B, Issler O, Pena CJ, et al. Alterations of the host microbiome affect behavioral responses to cocaine. *Sci Rep*. 2016;6:35455.
19. Cryan JF, Dinan TG. Mind-altering microorganisms: the impact of the gut microbiota on brain and behaviour. *Nat Rev Neurosci*. 2012;13:701–12.
20. Koh A, De Vadder F, Kovatcheva-Datchary P, Bäckhed F. From dietary fiber to host physiology: short-chain fatty acids as key bacterial metabolites. *Cell*. 2016;165:1332–45.
21. Frost G, Sleeth ML, Sahuri-Arisoylu M, Lizarbe B, Cerdan S, Brody L, et al. The short-chain fatty acid acetate reduces appetite via a central homeostatic mechanism. *Nat Commun*. 2014;5:3611.
22. Sampson TR, Debelius JW, Thron T, Janssen S, Shastri GG, Ilhan ZE, et al. Gut microbiota regulate motor deficits and neuroinflammation in a model of Parkinson’s disease. *Cell*. 2016;167:1469–80.e12.
23. Kratsman N, Getselter D, Elliott E. Sodium butyrate attenuates social behavior deficits and modifies the transcription of inhibitory/excitatory genes in the frontal cortex of an autism model. *Neuropharmacology*. 2016;102:136–45.
24. Davie JR. Inhibition of histone deacetylase activity by butyrate. *J Nutr*. 2003;133:2485S–93S.
25. Mews P, Egervari G, Nativio R, Sidoli S, Donahue G, Lombroso SI, et al. Alcohol metabolism contributes to brain histone acetylation. *Nature*. 2019;574:717–21.
26. Li X, Egervari G, Wang Y, Berger SL, Lu Z. Regulation of chromatin and gene expression by metabolic enzymes and metabolites. *Nat Rev Mol Cell Biol*. 2018;19:563–78.
27. Nankova BB, Agarwal R, MacFabe DF, La, Gamma EF. Enteric bacterial metabolites propionic and butyric acid modulate gene expression, including CREB-dependent catecholaminergic neurotransmission, in PC12 cells—possible relevance to autism spectrum disorders. *PLoS ONE*. 2014;9:e103740.
28. Shah P, Nankova BB, Parab S, La Gamma EF. Short chain fatty acids induce TH gene expression via ERK-dependent phosphorylation of CREB protein. *Brain Res*. 2006;1107:13–23.
29. Parab S, Nankova BB, La Gamma EF. Differential regulation of the tyrosine hydroxylase and enkephalin neuropeptide transmitter genes in rat PC12 cells by short chain fatty acids: concentration-dependent effects on transcription and RNA stability. *Brain Res*. 2007;1132:42–50.
30. Mally P, Mishra R, Gandhi S, Decastro MH, Nankova BB, Lagamma EF. Stereospecific regulation of tyrosine hydroxylase and proenkephalin genes by short-chain fatty acids in rat PC12 cells. *Pediatr Res*. 2004;55:847–54.
31. Goswami C, Iwasaki Y, Yada T. Short-chain fatty acids suppress food intake by activating vagal afferent neurons. *J Nutr Biochem*. 2018;57:130–5.
32. Lal S, Kirkup AJ, Brunnsden AM, Thompson DG, Grundy D. Vagal afferent responses to fatty acids of different chain length in the rat. *Am J Physiol Liver Physiol*. 2001;281:G907–15.
33. Fernandes AB, Alves da Silva J, Almeida J, Cui G, Gerfen CR, Costa RM, et al. Postingsitive modulation of food seeking depends on vagus-mediated dopamine neuron activity. *Neuron*. 2020;106:778–88.e6.
34. Dalile B, Van Oudenhove L, Vervliet B, Verbeke K. The role of short-chain fatty acids in microbiota–gut–brain communication. *Nat Rev Gastroenterol Hepatol*. 2019;16:461–78.
35. Taylor AMW, Castonguay A, Ghogha A, Vayssiere P, Pradhan AAA, Xue L, et al. Neuroimmune regulation of GABAergic neurons within the ventral tegmental area during withdrawal from chronic morphine. *Neuropsychopharmacology*. 2015;41:949.
36. Zhang L, Meng J, Ban Y, Jalodia R, Chupikova I, Fernandez I, et al. Morphine tolerance is attenuated in germfree mice and reversed by probiotics, implicating the role of gut microbiome. *Proc Natl Acad Sci USA*. 2019;116:13523 LP–32.
37. Kang M, Mischel RA, Bhawe S, Komla E, Cho A, Huang C, et al. The effect of gut microbiome on tolerance to morphine mediated antinociception in mice. *Sci Rep*. 2017;7:42658.
38. Simpson S, Kimbrough A, Boomhower B, McLellan R, Hughes M, Shankar K, et al. Depletion of the microbiome alters the recruitment of neuronal ensembles of oxycodone intoxication and withdrawal. *ENEURO*. 2020;7:ENEURO.0312-19.2020.
39. Callahan BJ, McMurdie PJ, Rosen MJ, Han AW, Johnson AJA, Holmes SP. DADA2: high-resolution sample inference from Illumina amplicon data. *Nat Methods*. 2016;13:581–3.
40. Bolyen E, Rideout JR, Dillon MR, Bokulich NA, Abnet CC, Al-Ghalith GA, et al. Reproducible, interactive, scalable and extensible microbiome data science using QIIME 2. *Nat Biotechnol*. 2019;37:852–7.
41. Quast C, Pruesse E, Yilmaz P, Gerken J, Schweer T, Yarza P, et al. The SILVA ribosomal RNA gene database project: improved data processing and web-based tools. *Nucleic Acids Res*. 2013;41:D590–6.
42. Dobin A, Davis CA, Schlesinger F, Drenkow J, Zaleski C, Jha S, et al. STAR: ultrafast universal RNA-seq aligner. *Bioinformatics*. 2013;29:15–21.
43. Ritchie ME, Phipson B, Wu D, Hu Y, Law CW, Shi W, et al. limma powers differential expression analyses for RNA-sequencing and microarray studies. *Nucleic Acids Res*. 2015;43:e47.
44. Torre D, Lachmann A, Ma’ayan A. BioJupies: automated generation of interactive notebooks for RNA-Seq data analysis in the cloud. *Cell Syst*. 2018;7:556–61.e3.
45. Raudvere U, Kolberg L, Kuzmin I, Arak T, Adler P, Peterson H, et al. g:Profiler: a web server for functional enrichment analysis and conversions of gene lists (2019 update). *Nucleic Acids Res*. 2019;47:W191–8.
46. Lu J, Synowicz S, Lu L, Yu Y, Bretherick T, Takada S, et al. Microbiota influence the development of the brain and behaviors in C57BL/6J mice. *PLoS ONE*. 2018;13:e0201829.
47. Banerjee S, Sindberg G, Wang F, Meng J, Sharma U, Zhang L, et al. Opioid-induced gut microbial disruption and bile dysregulation leads to gut barrier compromise and sustained systemic inflammation. *Mucosal Immunol*. 2016;9:1418–28.
48. Wang F, Meng J, Zhang L, Johnson T, Chen C, Roy S. Morphine induces changes in the gut microbiome and metabolome in a morphine dependence model. *Sci Rep*. 2018;8:3596.
49. Lee K, Vuong HE, Nusbaum DJ, Hsiao EY, Evans CJ, Taylor AMW. The gut microbiota mediates reward and sensory responses associated with regimen-selective morphine dependence. *Neuropsychopharmacology*. 2018;43:2606–14.
50. Louis P, Flint HJ. Formation of propionate and butyrate by the human colonic microbiota. *Environ Microbiol*. 2017;19:29–41.
51. Louis P, Flint HJ. Diversity, metabolism and microbial ecology of butyrate-producing bacteria from the human large intestine. *FEMS Microbiol Lett*. 2009;294:1–8.
52. Douglas GM, Maffei VJ, Zaneveld J, Yurgel SN, Brown JR, Taylor CM, et al. PICRUSt2: an improved and extensible approach for metagenome inference. *BioRxiv*. 2019. <https://doi.org/10.1101/672295>.
53. Zito KA, Vickers G, Roberts DC. Disruption of cocaine and heroin self-administration following kainic acid lesions of the nucleus accumbens. *Pharm Biochem Behav*. 1985;23:1029–36.
54. Kelsey JE, Carlezon WA, Falls WA. Lesions of the nucleus accumbens in rats reduce opiate reward but do not alter context-specific opiate tolerance. *Behav Neurosci*. 1989;103:1327–34.
55. Lachmann A, Xu H, Krishnan J, Berger SI, Mazloom AR, Ma’ayan A. ChEA: transcription factor regulation inferred from integrating genome-wide ChIP-X experiments. *Bioinformatics*. 2010;26:2438–44.
56. Chen EY, Tan CM, Kou Y, Duan Q, Wang Z, Meirilles GV, et al. Enrichr: interactive and collaborative HTML5 gene list enrichment analysis tool. *BMC Bioinform*. 2013;14:128.
57. Kuleshov MV, Jones MR, Rouillard AD, Fernandez NF, Duan Q, Wang Z, et al. Enrichr: a comprehensive gene set enrichment analysis web server 2016 update. *Nucleic Acids Res*. 2016;44:W90–7.
58. Hulsen T, de Vlieg J, Alkema W. BioVenn—a web application for the comparison and visualization of biological lists using area-proportional Venn diagrams. *BMC Genom*. 2008;9:488.
59. Nanda JS, Kumar R, Raghava GPS. dbEM: a database of epigenetic modifiers curated from cancerous and normal genomes. *Sci Rep*. 2016;6:19340.

60. Smith PM, Howitt MR, Panikov N, Michaud M, Gallini CA, Bohlooly-Y M, et al. The microbial metabolites, short-chain fatty acids, regulate colonic Treg cell homeostasis. *Science*. 2013;341:569–73.
61. Waldecker M, Kautenburger T, Daumann H, Busch C, Schrenk D. Inhibition of histone-deacetylase activity by short-chain fatty acids and some polyphenol metabolites formed in the colon. *J Nutr Biochem*. 2008;19:587–93.
62. Soliman ML, Rosenberger TA. Acetate supplementation increases brain histone acetylation and inhibits histone deacetylase activity and expression. *Mol Cell Biochem*. 2011;352:173–80.
63. Fellows R, Denizot J, Stellato C, Cuomo A, Jain P, Stoyanova E, et al. Microbiota derived short chain fatty acids promote histone crotonylation in the colon through histone deacetylases. *Nat Commun*. 2018;9:105.
64. Hoban AE, Stilling RM, Moloney G, Shanahan F, Dinan TG, Clarke G, et al. The microbiome regulates amygdala-dependent fear recall. *Mol Psychiatry*. 2018;23:1134–44.
65. Bardo MT, Bevins RA. Conditioned place preference: what does it add to our preclinical understanding of drug reward? *Psychopharmacology*. 2000;153:31–43.
66. Kim S, Kaang B-K. Epigenetic regulation and chromatin remodeling in learning and memory. *Exp Mol Med*. 2017;49:e281.
67. Sanchis-Segura C, Lopez-Atalaya JP, Barco A. Selective boosting of transcriptional and behavioral responses to drugs of abuse by histone deacetylase inhibition. *Neuropsychopharmacology*. 2009;34:2642.
68. Sheng J, Lv gang Z, Wang L, Zhou Y, Hui B. Histone H3 phosphoacetylation is critical for heroin-induced place preference. *Neuroreport*. 2011;22:575–80.